Fabrication of Multiresponsive Shell Cross-Linked Micelles Possessing pH-Controllable Core Swellability and Thermo-Tunable Corona Permeability

Xiaoze Jiang, Zhishen Ge, Jian Xu, Hao Liu, and Shiyong Liu*

Department of Polymer Science and Engineering, Hefei National Laboratory for Physical Sciences at the Microscale, University of Science and Technology of China, Hefei, Anhui 230026, China

A double hydrophilic ABC triblock copolymer, poly(2-(diethylamino)ethyl methacrylate)-*b*-poly(2-(dimethylamino)-ethyl methacrylate)-*b*-poly(*N*-isopropylacrylamide) (PDEA-*b*-PDMA-*b*-PNIPAM), containing the well-known pH-responsive PDEA block and thermoresponsive PNIPAM block, was synthesized by atom transfer radical polymerization via sequential monomer addition using ethyl 2-chloropropionate as the initiator. The obtained triblock copolymer exhibits interesting "schizophrenic" micellization behavior in aqueous solution, and supramolecularly self-assembles into three-layer "onion-like" PNIPAM-core micelles at acidic pH's and elevated temperatures and PDEA-core micelles with "inverted" structures at alkaline pH's and room temperature. In both cases, dynamic laser light scattering (LLS) and optical transmittance reveal the presence of near-monodisperse micelles, and the micelle formation/inversion process is fully reversible. Novel shell cross-linked (SCL) micelles with pH-responsive PDEA cores and thermoresponsive PNIPAM coronas were then facilely fabricated from the PDEA-*b*-PDMA-*b*-PNIPAM triblock copolymer by cross-linking the PDMA inner shells with 1,2-bis(2-iodoethoxy)-ethane. The reversible pH-dependent swelling/shrinking of PDEA cores and thermosensitive collapse/aggregation of PNIPAM coronas of the obtained SCL micelles were investigated in detail by dynamic LLS, optical transmittance, and transmission electron microscopy. As the structurally stable SCL micelles possess pH-controllable core swellability and thermo-tunable corona permeability, the release profile of a model hydrophobic drug, dipyridamole, initially loaded within the hydrophobic PDEA core, can be dually controlled by both the solution pH and the temperature. This represents the first report of SCL micelles with multiresponsive cores and coronas, which may find practical applications in fields such as drug delivery and smart release.

Introduction

Water-soluble double hydrophilic block copolymers (DHBCs) exhibit intriguing "schizophrenic" micellization behavior, self-assembling into two or more types of micelles with invertible structures under a combination of external stimuli such as pH, temperature, and ionic strengths.[1−18] Poly(*N*-isopropylacrylamide) (PNIPAM)[3,4,16,17] and poly(propylene oxide) (PPO)[11,18] have been frequently used as the thermosensitive components, while poly(2-(diethylamino)ethyl methacrylate) (PDEA),[8,11,14,18] poly(acrylic acid) (PAA),[5,9,17] poly(methacrylic acid) (PMAA),[12] and poly(4-vinyl pyridine) (P4VP)[9,16] can act as the pH-responsive blocks. Various diblock copolymers based on combinations of the above stimuli-responsive blocks have been extensively studied.

Recently, growing attention has been paid to schizophrenic triblock copolymers, providing enhanced structural versatility and additional aggregation modes.[16,19,20] Armes and co-workers synthesized a poly(ethylene oxide)-*b*-poly(2-(diethylamino)ethyl methacrylate)-*b*-poly(2-hydroxyethyl methacrylate) (PEO-*b*-PDEA-*b*-PHEMA) triblock copolymer and further converted the PHEMA block into poly(2-succinyloxyethyl methacrylate) (PSEMA) by esterification with succinic anhydride. The obtained PEO-*b*-PDEA-*b*-PSEMA triblock copolymer can self-assemble into a "trinity" of micellar aggregates in aqueous solution simply by adjusting the solution pH at ambient

temperature.[19] Zhang et al. reported the schizophrenic micellization of PEO-*b*-P4VP-*b*-PNIPAM; the presence of PEO provides additional stabilization of the P4VP-core and PNIPAM-core micelles formed under a combination of pH and temperature.[16]

However, the practical applications of various self-assembled aggregates of DHBCs were limited by their structural instability upon dilution or changes of external conditions. The approaches of core cross-linking[21−26] or shell cross-linking[27−30] of micelles were then developed to maintain their structural integrity. The latter approach was originally reported by Wooley et al. for amphiphilic block copolymers.[31−33] Armes and co-workers then applied this method to the structural fixation of DHBC micelles[34,35] and further developed the triblock copolymer approach for the preparation of shell cross-linked (SCL) micelles at high solids, taking advantage of steric stabilization of the soluble block located in the outer coronas of three-layer "onion-like" micelles.[36−38]

However, all of the previously reported SCL micelles of DHBCs possessed neutral coronas such as PEO,[36−41] poly(oligo-(ethylene glycol) methyl ether methacrylate) (POEGMA),[42] poly(*N,N*-dimethylacrylamide),[43] or poly(glycerol monomethacrylate) (PGMA),[44] although the micelle cores were pH- or thermoresponsive. In practical applications such as targeted drug delivery, tunable release, recyclable catalysts, and smart separation, SCL micelles possessing stimuli-responsive coronas would be highly desirable.

Tang et al. investigated the pH-induced micellization behavior of PEO-*b*-PDMA-*b*-PDEA, where PDMA is poly(2-(dimethyl-

amino)ethyl methacrylate). They also solubilized a model hydrophobic drug, dipyridamole (DIP), within the PDEA cores and found that the release kinetics of DIP can be triggered by the pH, leading to reversible micelle formation/disintegration.[45] However, the burst release of DIP at low pH's due to micelle dissociation may be unfavorable in certain cases. Moreover, the issue of micelle stability during circulation in the blood compartments, typically accompanied by a large dilution, should also be considered.

In terms of the practical applications such as drug delivery and controlled release, this novel type of intriguing nanocarrier with pH-triggered releasing ability can be further developed based on the following principles. First, shell cross-linking can maintain the structural integrity of micelles, while keeping the encapsulation capacity of the hydrophobic PDEA cores. It should be noted that shell cross-linking can also partially modulate the release of guest molecules. Second, if we replace the neutral PEO outer corona of the obtained SCL micelles with a stimuli-responsive one, such as PNIPAM, the permeability of the corona can be tuned by the reversible thermal phase transitions above or below its lower critical solution temperature (LCST). The solvation or collapse/aggregation of the PNIPAM corona will then retard or accelerate the diffusion of guest molecules out of the nanocarriers.[46,47] Finally, the combination of pH-controlled swellability of the PDEA core and thermo-induced corona permeability can exhibit dual control over the release profiles of guest molecules, leading to more sophisticated and smarter drug nanocarriers.

Herein, we report the synthesis of a novel double hydrophilic triblock copolymer, poly(2-(diethylamino)ethyl methacrylate)-*b*-poly(2-(dimethylamino)ethyl methacrylate)-*b*-poly(*N*-isopropylacrylamide) (PDEA-*b*-PDMA-*b*-PNIPAM) via sequential atom transfer radical polymerization (ATRP). It can self-assemble into PDEA-core micelles at alkaline pH's and room temperature and PNIPAM-core micelles at acidic pH's and elevated temperatures. The PDEA-core micelles possess a three-layer onion-like structure, with PDMA and PNIPAM blocks forming the inner layers and outer coronas, respectively. Cross-linking of the PDMA inner layer leads to the formation of structurally stable SCL micelles, which possess pH-responsive PDEA cores and thermoresponsive PNIPAM coronas. Using DIP as a model hydrophobic drug, we successfully demonstrate that the release of encapsulated guest molecules within the PDEA core of SCL micelles can be dually controlled by solution pH and temperature. The latter two factors can finely tune the extent of swelling/shrinking of PDEA cores and the permeability of PNIPAM coronas to model drugs, respectively.

Experimental Section

Materials. 2-(Dimethylamino)ethyl methacrylate (DMA, 99%, Aldrich) and 2-(diethylamino)ethyl methacrylate (DEA, 99%, Aldrich) were dried over calcium hydride, vacuum-distilled, and then stored at −20 °C prior to use. *N*-Isopropylacrylamide (NIPAM, 97%, Tokyo Kasei Kagyo Co.) was recrystallized from a mixture of benzene and *n*-hexane (1:3 (v/v)). CuCl, ethyl 2-chloropropionate (ECP), 1,2-bis-(2-iodoethoxy)ethane (BIEE), tris(aminoethyl)amine (TREN), 2,2′-bipyridine (bpy), and dipyridamole (DIP) were purchased from Aldrich and used as received. Tris(2-(dimethylamino)ethyl)amine (Me6TREN) was prepared from TREN according to literature procedures.[48] Isopropyl alcohol (IPA), *n*-hexane, ethyl ether, and all other chemicals were purchased from Shanghai Chemical Reagent Co. and used as received.

Sample Synthesis. *Preparation of PDEA-b-PDMA-Cl Macroinitiator.* A reaction flask with a magnetic stirrer and a rubber septum was charged with ECP (64 μL, 0.5 mmol), DEA (2.97 g, 16 mmol),

bpy (156 mg, 1.0 mmol), and IPA (3.5 mL). The flask was degassed by three freeze−pump−thaw cycles, back-filled with N2, and then placed in an oil bath thermostated at 40 °C. After ∼5 min, CuCl (49 mg, 0.5 mmol) was added to start the polymerization under a N2 atmosphere. After 6 h, the DEA conversion reaches ≥98%, as judged by ^{1}H NMR sampled at time intervals. An aliquot of the reaction mixture was withdrawn for subsequent gel permeation chromatography (GPC) analysis before the introduction of a degassed mixture of DMA monomer (5.50 g, 35 mmol) and IPA (6.0 mL) via a double-tipped needle. After 5 h, the reaction flask was quenched in liquid nitrogen, exposed to air, and diluted with 10 mL of IPA. After passing though a silica gel column to remove the copper catalysts and removing all the solvent by a rotary evaporator, the residues were dissolved in tetrahydrofuran (THF) and precipitated into cold *n*-hexane (−70 °C) to remove residual monomers. After the supernatant solution was discarded, the product was collected as colorless and viscous solids. It was then dried in a vacuum oven overnight at room temperature. The overall yield was ∼80%. GPC analysis of PDEA-*b*-PDMA-Cl revealed an M_n of 16 700 and a polydispersity, M_w/M_n, of 1.21. The PDEA content in the diblock copolymer was determined to be 32 mol % by ^{1}H NMR. Thus, the degrees of polymerization (DPs) of PDEA and PDMA blocks were estimated to be 31 and 66, respectively. The diblock copolymer was thus denoted PDEA31-*b*-PDMA66-Cl.

Preparation of PDEA-b-PDMA-b-PNIPAM Triblock Copolymer. The triblock copolymer was synthesized by ATRP polymerization of NIPAM monomer using PDEA31-*b*-PDMA66-Cl as the macroinitiator. A typical procedure was as follows. NIPAM (1.47 g, 13 mmol), Me6-TREN (23 mg, 0.1 mmol), PDEA31-*b*-PDMA66-Cl (1.67 g, 0.1 mmol), and 2-propanol (4 mL) were charged into a 25 mL reaction flask. The reaction mixture was degassed by two freeze−pump−thaw cycles and back-filled with N2. After the reaction mixture was warmed to room temperature, CuCl (10 mg, 0.1 mmol) was introduced into the reaction flask under the protection of N2 flow. After polymerization at room temperature under N2 atmosphere for 10 h, the flask was quenched in liquid nitrogen, exposed to air, and then diluted with 5 mL of 2-propanol. After passing through a silica gel column to remove the copper catalysts and removing all of the solvent, the obtained solids were thoroughly washed with an excess of *n*-hexane and ethyl ether successively to remove the possible presence of residual NIPAM monomer and unreacted PDEA-*b*-PDMA macroinitiator, respectively. The obtained colorless product was dried in a vacuum oven overnight at room temperature. The overall yield was ∼70%. The residual copper in PDEA-*b*-PDMA-*b*-PNIPAM was determined to be ∼15 ppm by atomic absorption spectrometry. GPC analysis of the obtained PDEA-*b*-PDMA-*b*-PNIPAM triblock copolymer revealed an M_n of 31 200 and an M_w/M_n of 1.29. The actual DP of the PNIPAM block was determined to be 106 by ^{1}H NMR analysis in CDCl3. The triblock copolymer was then denoted PDEA31-*b*-PDMA66-*b*-PNIPAM106.

Preparation of Micelles and SCL Micelles. At room temperature, the PDEA-*b*-PDMA-*b*-PNIPAM triblock copolymer was dissolved in water at a concentration of 10.0 g/L and pH 4−5. The solution pH was adjusted to 9.0 with the slow addition of concentrated NaOH aqueous solution to induce the formation of PDEA-core micelles.

Subsequent shell cross-linking of PDEA-core micelles was achieved by the addition of BIEE. The solution mixture was stirred for 3 days at room temperature. The [BIEE]/[DMA] molar ratio was fixed at 1:2, targeting a 100% degree of cross-linking.

Loading SCL Micelles with DIP. DIP (15.0 mg) was added to 20 mL of the obtained SCL micelles at a concentration of 5.0 g/L. Adjusting the solution pH to 4−5 allows the complete dissolution of DIP. After being stirred for 5 min, the solution pH was adjusted to 9.0 with the addition of NaOH. The drug-loaded SCL micellar solution was equilibrated for 20 min at room temperature and then filtered through a 0.45 μm Millipore filter to remove any non-encapsulated DIP. However, UV−vis absorbance analysis of the filtrate (after dilution

Scheme 1. Synthesis of the PDEA$_{31}$-*b*-PDMA$_{66}$-*b*-PNIPAM$_{106}$ Triblock Copolymer
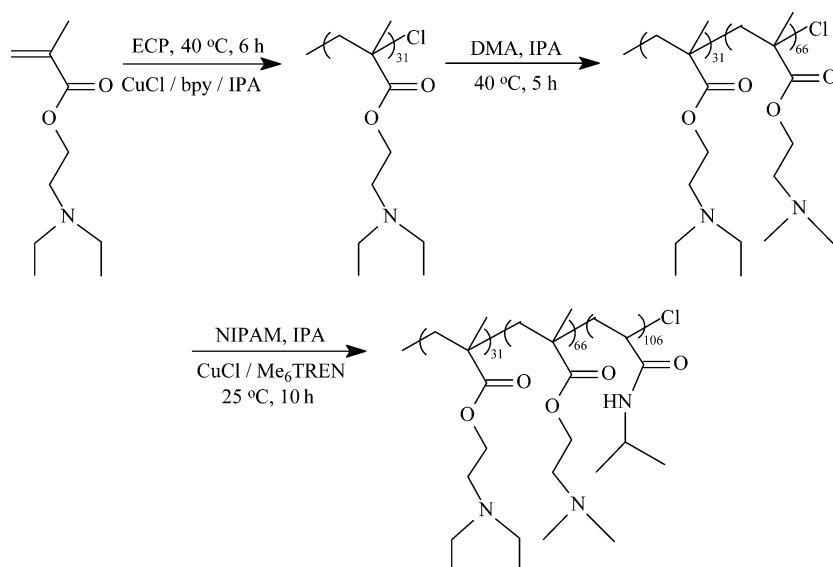
with water and adjusting back to pH 3.0) at 284 nm based on a standard curve for DIP at pH 3.0 revealed that all of the added DIP was encapsulated within the micelle core. This is reasonable considering that for the encapsulation of DIP within the non-cross-linked micelles of PEO-*b*-PDMA-*b*-PDEA the loading content can be as high as 20% (w/w).[45]

In Vitro Drug Release. Four parallel time-dependent drug release experiments were conducted at the same time. A 2 mL aqueous solution of SCL micelles solubilized with 15% (w/w) DIP was transferred into dialysis tubes with a molecular weight cutoff of 14 000 and then immersed into 50 mL buffer solutions at four types of different conditions: pH 8.0 and 25 °C, pH 8.0 and 37 °C, pH 5.0 and 25 °C, pH 5.0 and 37 °C. Aliquots (3.0 mL) of the buffer solutions were taken at time intervals. The solution was further diluted, adjusted to pH 3.0, and then monitored by UV−vis spectroscopy at 284 nm to determine the rate of drug release. Meanwhile, 3.0 mL of fresh buffer was added after each sampling to keep the total volume of buffer solutions constant. Cumulative release is expressed as the total percentage of drug released through the dialysis membrane over time.

Characterization. Molecular weights and molecular weight distributions were determined by GPC with a Waters 1515 pump and a Waters 2414 differential refractive index detector (set at 30 °C). It employs a series of three linear Styragel columns HT2, HT4, and HT5 and an oven temperature of 45 °C. The eluent was THF at a flow rate of 1.0 mL/min. A series of low polydispersity polystyrene standards was employed for the GPC calibration.

All ^{1}H NMR spectra were recorded in D$_2$O or CDCl$_3$ using a Bruker 300 MHz spectrometer. The UV−vis spectra and transmittance were acquired on a Unico UV−vis 2802PCS spectrophotometer. The transmittance of the solution was measured at a wavelength of 500 nm using a thermostatically controlled cuvette.

A commercial spectrometer (ALV/DLS/SLS-5022F) equipped with a multi-tau digital time correlator (ALV5000) and a cylindrical 22 mW UNIPHASE He−Ne laser (λ_0 = 632 nm) as the light source was employed for dynamic laser light scattering (LLS) measurements. Scattered light was collected at a fixed angle of 90° for a duration of 10 min. Distribution averages and particle size distributions were computed using cumulants analysis and CONTIN routines. All data were averaged over three measurements.

Transmission electron microscopy (TEM) images were recorded using a Philips CM120 electron microscope at an accelerating voltage of 200 kV. TEM samples were prepared by placing 10 μL aqueous solutions of SCL micelles (0.2 g/L) on copper grids coated with thin films of Formvar and carbon. No staining was required.

Results and Discussion

Synthesis of PDEA-*b*-PDMA-*b*-PNIPAM Triblock Copolymer. The ATRP technique is very tolerant of monomer functionalities and can be conveniently employed for the preparation of a wide variety of amphiphilic[49−51] and double hydrophilic block copolymers.[10,52,53] The controlled ATRP of DEA and DMA monomers and the facile preparation of PDEA-*b*-PDMA block copolymers by sequential monomer addition in methanol or IPA using CuX/bpy catalysts have been well-documented.[19,38,42,44,54,55] However, the controlled ATRP of acrylamido monomers including NIPAM has once been a challenge due to problems such as the deactivation of the copper catalyst through complexation with amide groups, displacement of the terminal halide atom by amides groups, and low values of the ATRP equilibrium constant.[56] Recent progress in the controlled ATRP of NIPAM was reported by Stöver and co-workers.[57,58] The combination of more active CuCl/Me$_6$TREN catalysts, alkyl chloride initiator, and IPA solvent in the polymerization system can overcome these problems, leading to the facile preparation at room temperature of PNIPAM with good conversion, controlled molecular weight, and narrow polydispersity.

Thus, a two-step approach was employed for the preparation of the PDEA-*b*-PDMA-*b*-PNIPAM triblock copolymer, the PDEA-*b*-PDMA diblock copolymer was synthesized in IPA at 40 °C by sequential monomer addition using CuCl/bpy catalysts and ECP as the ATRP initiator, and the obtained PDEA-*b*-PDMA-Cl was then employed as a macroinitiator for the ATRP polymerization of NIPAM in IPA at room temperature using CuCl/Me$_6$TREN catalysts (Scheme 1).

During the preparation of the PDEA-*b*-PDMA-Cl macroinitiator, the DEA monomer was polymerized first, and the monomer conversion was monitored by ^{1}H NMR. After 6 h, the DEA conversion was greater than 98%. GPC analysis of samples withdrawn at this stage revealed a monomodal and symmetric peak with an M_n of 6100 and an M_w/M_n of 1.17 (Figure 1). A degassed mixture of DMA monomer and IPA was then transferred into the reaction flask to start the chain extension of the second block. After 5 h, the polymerization was stopped, and residual monomer was removed by precipitation of the product from THF into cold *n*-hexane. In comparison to the GPC trace of the first PDEA block just before addition
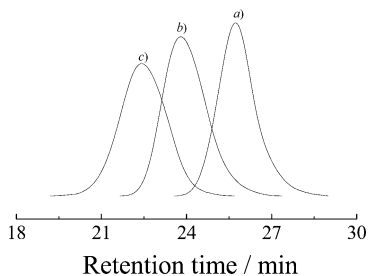
Figure 1. THF GPC traces of (a) PDEA precursor (M_n = 6100, M_w/M_n = 1.17), (b) PDEA-*b*-PDMA-Cl macroinitiator (M_n = 16 700, M_w/M_n = 1.21), and (c) PDEA-*b*-PDMA-*b*-PNIPAM triblock copolymer (M_n = 31 200, M_w/M_n = 1.29).
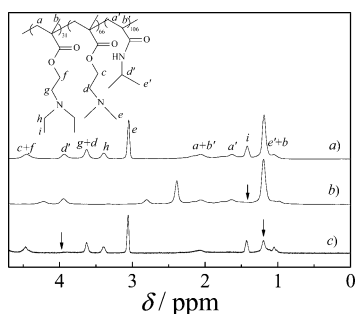

Figure 2. ^{1}H NMR spectra of the PDEA-*b*-PDMA-*b*-PNIPAM triblock copolymer in D$_2$O: (a) at pH 5.0 and 25 °C; (b) at pH 9.0 and 25 °C; (c) at pH 5.0 and 40 °C.

of the DMA monomer, the elution peak of PDEA-*b*-PDMA-Cl clearly shifted to a larger molecular weight, with an M_n of 16 700 and an M_w/M_n of 1.21 (Figure 1). Moreover, there is no tailing at the lower-molecular-weight side, indicating a successful chain extension of the second PDMA block. The PDEA content in the PDEA-*b*-PDMA-Cl diblock copolymer was determined to be 32% by ^{1}H NMR in CDCl$_3$. The DPs of the PDEA and PDMA blocks were estimated to be 31 and 66, respectively, based on the chemical composition and molecular weight determined from GPC.

The obtained PDEA$_{31}$-*b*-PDMA$_{66}$-Cl diblock copolymer was then employed as a macroinitiator for the ATRP polymerization of the NIPAM monomer in IPA at room temperature, employing the CuCl/Me$_6$TREN catalysts, leading to the preparation of PDEA-*b*-PDMA-*b*-PNIPAM triblock copolymer. The ^{1}H NMR spectrum of the purified product in D$_2$O at pH 5.0 (Figure 2a) reveals the presence of characteristic signals of all three blocks. The DP of the PNIPAM block was determined to be 106 by ^{1}H NMR, based on the integral ratio of resonances at 3.9 ppm (d′) and 4.4 ppm (c and f), characteristic of PNIPAM and PDMA/PDEA blocks, respectively.

Most importantly, in comparison to the GPC trace obtained for the PDEA-*b*-PDMA diblock precursor, there is a clear shift to a higher molecular weight for the PDEA-*b*-PDMA-*b*-PNIPAM triblock copolymer (Figure 1c). The elution peak of the triblock copolymer is also symmetric and shows no tailing at the lower-molecular-weight side, suggesting a high initiating efficiency of the macroinitiator for the polymerization of NIPAM and a successful preparation of the target triblock copolymer. GPC analysis revealed an M_n of 31 200 and an M_w/M_n of 1.29.

Schizophrenic Micellization of PDEA-*b*-PDMA-*b*-PNIPAM. Both PDMA and PDEA are weak polybases, and their conjugated acids have pK_a's of 7.0 and 7.3, respectively.[38,59−62] At room temperature, the PDMA homopolymer is water-soluble over the whole pH range with a slightly lower water solubility at pH > 9−10. In contrast, the PDEA homopolymer is water-insoluble at neutral or alkaline pH's. Below pH 6−7, it is soluble as a weak cationic polyelectrolyte due to the protonation of tertiary amine groups. However, the PNIPAM homopolymer dissolves in cold and dilute aqueous solutions but becomes insoluble above ∼32 °C due to the LCST phase behavior. Thus, it was quite expected that the PDEA-*b*-PDMA-*b*-PNIPAM triblock copolymer will exhibit thermo- and pH-responsive schizophrenic micellization behavior in aqueous solution (Scheme 2). For the aqueous solution of PDEA-*b*-PDMA-*b*-PNIPAM at a concentration of 5.0 g/L, it was clear at pH 5.0 and room temperature. Upon heating the solution to 40 °C at pH 5.0 or

Scheme 2. Schizophrenic Micellization Behavior of the PDEA-*b*-PDMA-*b*-PNIPAM Triblock Copolymer in Aqueous Solution (Top) and the Subsequent Fabrication of Multiresponsive SCL Micelles (Bottom)
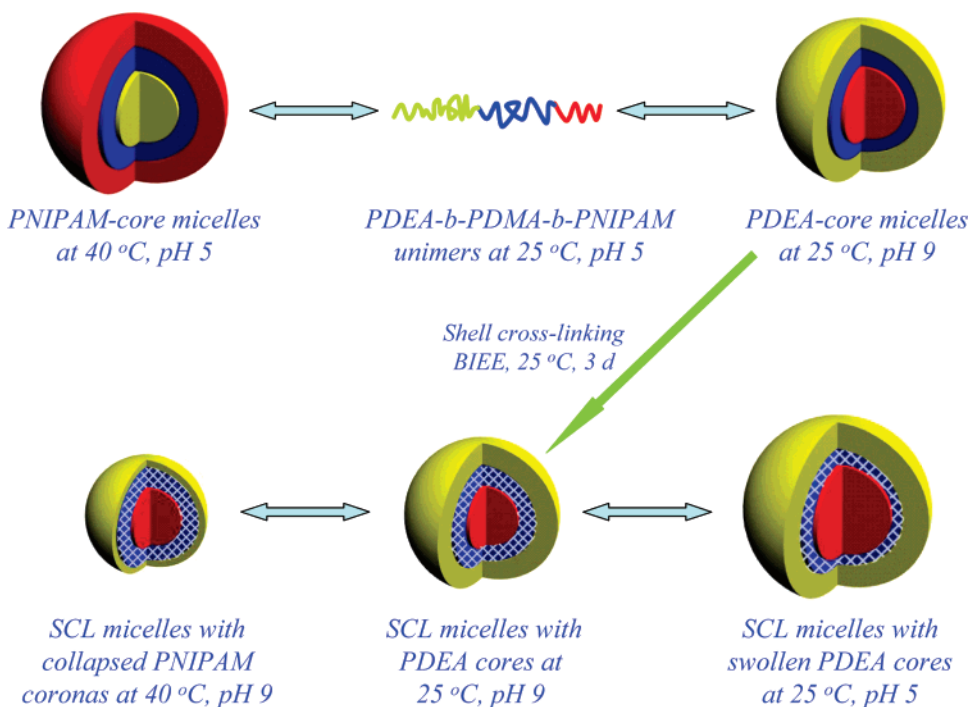

PNIPAM-core micelles at 40 °C, pH 5

PDEA-b-PDMA-b-PNIPAM unimers at 25 °C, pH 5

PDEA-core micelles at 25 °C, pH 9

Shell cross-linking BIEE, 25 °C, 3 d

SCL micelles with collapsed PNIPAM coronas at 40 °C, pH 9

SCL micelles with PDEA cores at 25 °C, pH 9

SCL micelles with swollen PDEA cores at 25 °C, pH 5

Figure 3. Digital photographs obtained for 5.0 g/L aqueous solutions of PDEA-*b*-PDMA-*b*-PNIPAM and SCL micelles at different pH's and temperatures.

adjusting to pH 9.0 at 25 °C, we can clearly observe the large increase of light scattering and the appearance of the bluish tinge characteristic of colloidal dispersion (Figure 3). This apparently indicates that the triblock copolymer can exhibit thermo- and pH-responsive micellization. ^{1}H NMR and dynamic LLS were further employed to characterize the micelle structures.

Figure 2 shows the ^{1}H NMR spectra of PDEA-*b*-PDMA-*b*-PNIPAM in D$_2$O at different conditions. At pH 5.0 and 25 °C, all signals characteristic of PNIPAM, PDMA, and PDEA blocks are visible, indicating that the triblock copolymer molecularly dissolves. Upon increasing the temperature to 40 °C at pH 5.0, the intensities of characteristic PNIPAM signals at $\delta = 3.9$ and 1.2 ppm decrease to a large extent (Figure 2c), indicating that the PNIPAM block becomes insoluble above its LCST. However, the characteristic signals of the PDMA and PDEA blocks at $\delta = 1.4$ and 4.4 ppm are clearly evident, which is reasonable as these two blocks are soluble at pH 5.0 due to the protonation of tertiary amine residues. On the basis of chemical intuition, three-layer onion-like micelles consisting PNIPAM cores, protonated PDMA inner layers, and protonated PDEA outer coronas should form at pH 5.0 and 40 °C (Scheme 2). It should be noted that the characteristic PNIPAM signals do not completely disappear. This suggests that the PNIPAM core remains partially solvated even at 40 °C; i.e., the micelle core still contains solvent molecules. This is similar to the case of thermoresponsive micellization of PPO-containing block co-polymers.[63−65] Hurter et al.[66] also theoretically predicted the presence of water in the micellar core in their modeling of the thermo-induced micellization of Pluronics.

Starting from the monomer state at pH 5.0 and 25 °C, signals characteristic of the PDEA block at 1.4 ppm completely disappeared upon adjusting to pH 9.0 at room temperature (Figure 2b), while signals characteristic of PNIPAM and PDMA at $\delta = 3.9$ and 2.4 ppm, respectively, are still clearly visible. This indicates the formation of structurally inverted onion-like micelles consisting of PDEA cores, PDMA inner shells, and PNIPAM coronas, compared to those formed at pH 5.0 and 40 °C (Scheme 2).

Figure 4a shows the temperature dependence of dynamic LLS results for the PDEA-*b*-PDMA-*b*-PNIPAM triblock copolymer at pH 5.0 and a concentration of 1.0 g/L. Below 34 °C, the average hydrodynamic radius, $\langle R_h \rangle$, is ∼9−10 nm, and the scattered light intensity is quite low, confirming that the triblock copolymer molecularly dissolves. Above 34 °C, $\langle R_h \rangle$ starts to
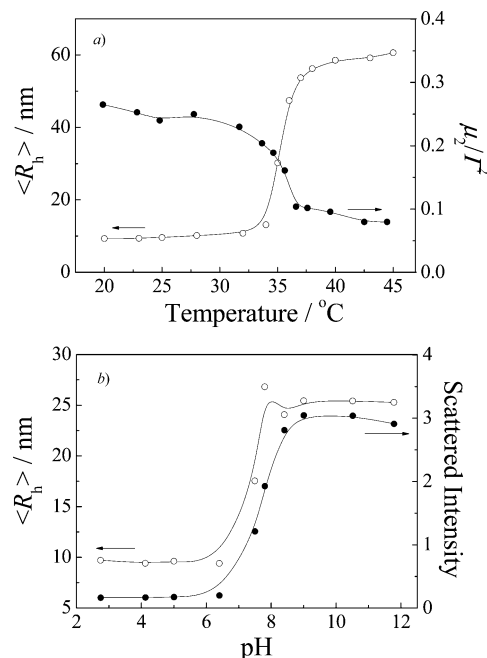

Figure 4. (a) Variation of intensity-average hydrodynamic radius, $\langle R_h \rangle$, and polydispersity index, μ_2/Γ^2, with temperature obtained for 1.0 g/L aqueous solutions of PDEA-*b*-PDMA-*b*-PNIPAM at pH 5.0. (b) Variation of $\langle R_h \rangle$ and scattered light intensity as a function of pH obtained for 1.0 g/L aqueous solutions of the PDEA-*b*-PDMA-*b*-PNIPAM triblock copolymer at 25 °C.

increase with temperature, accompanied by an increase of scattered light intensity, suggesting thermoresponsive micelli-zation above the critical micellization temperature due to the thermal phase transition of PNIPAM block. Above 38 °C, dynamic LLS only revealed one population, and $\langle R_h \rangle$ remains almost constant at ∼60 nm. This indicates that the thermo-induced micellization is complete. Moreover, the formed PNIPAM-core micelles are quite monodisperse, with polydis-persities (μ_2/Γ^2) typically less than 0.10 (Scheme 2).

Figure 4b shows the pH dependence of dynamic LLS results for PDEA-*b*-PDMA-*b*-PNIPAM. Below pH 6−7, the triblock copolymer molecularly dissolves, with very low scattering intensity. Upon addition of NaOH, micellization occurred above pH 7, as indicated by the appearance of a bluish tinge that is characteristic of micellar solutions. Above pH 8, the micelle size remains almost constant, with $\langle R_h \rangle$ of ∼25 nm. The size distribution is relatively monodisperse, with a μ_2/Γ^2 of 0.09. This agrees quite well with the previous ^{1}H NMR results. Further studies indicated that the thermo- and pH-induced micellization of PDEA-*b*-PDMA-*b*-PNIPAM triblock copolymer is fully reversible, and the schizophrenic micellization behavior is summarized in Scheme 2.

Shell Cross-Linked Micelles with Multiresponsive Cores and Coronas. In alkaline media and at room temperature, the self-assembled three-layer onion-like micelles consist of PDEA cores, PDMA inner shells, and PNIPAM outer coronas. Thus, the PDEA core and PNIPAM corona possess pH- and thermo-responsiveness. To combine these two intriguing properties and avoid structural disintegration or inversion, the shell cross-linking of the inner PDMA layer was then facilitated upon addition of a difunctional cross-linker, BIEE. It can selectively quaternize the DMA residues and leads to successful "locking in" of the micelle structure (Scheme 2).[34−36,38] The molar ratio of BIEE to DMA residues was 1:2, targeting a 100% degree of cross-linking. The actual degree of quaternization of SCL micelles was determined to be ∼70% by ^{1}H NMR analysis in
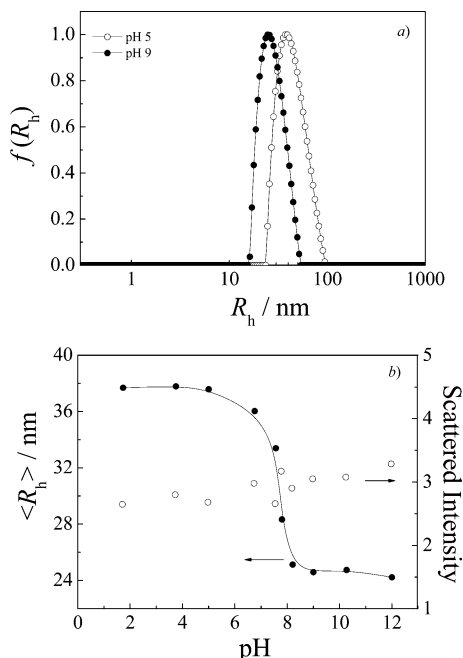
Figure 5. (a) Typical hydrodynamic radius distribution, $f(R_h)$, at pH 5.0 and 9.0, and (b) variation of intensity-average hydrodynamic radius, $\langle R_h \rangle$, and scattered light intensity at a scattering angle of 90° as a function of pH obtained for 1.0 g/L aqueous solutions of SCL micelles of the PDEA-*b*-PDMA-*b*-PNIPAM triblock copolymer. The target degree of shell cross-linking was 100%.

D_2O (pH 9) by comparing the integration areas of signals characteristic of unquaternized DMA residues at $\delta = 2.4$ ppm to that of PNIPAM residues at $\delta = 3.9$ ppm.

After shell cross-linking, the solution pH was adjusted back to pH 5.0, we can clearly observe that the bluish tinge persists (Figure 3), and this apparently indicates that the shell cross-linking is successful. Otherwise, the micelle dissociation at acidic pH will lead to the disappearance of the bluish tinge and a clear solution. The structures of the obtained SCL micelles and the properties of multiresponsiveness of the micelle cores and coronas were further investigated by dynamic LLS and TEM.

Typical hydrodynamic radius distributions, $f(R_h)$, of the obtained SCL micelles at pH 5.0 and 9.0 are shown in Figure 5a. Both size distributions are relatively narrow, with μ_2/Γ^2 values being 0.15 and 0.11 for SCL micelles at pH 5.0 and 9.0, respectively. Most importantly, the intensity-average hydrodynamic radius, $\langle R_h \rangle$, at pH 5.0 is much larger than that at pH 9.0, being 38 and 24 nm, respectively. This suggests that upon the pH increase from 5.0 to 9.0 the hydrodynamic volume of the SCL micelles shrinks ~4 times. The size increase at low pH should be due to the protonation and swelling of the PDEA cores. The pH-induced swelling/deswelling of PDEA cores of SCL micelles has been reported previously.[37,38,40]

The SCL micelles exhibit a $\langle R_h \rangle$ of ~24 nm at pH 9.0, which is almost the same as that obtained for the non-cross-linked micelles. The polydispersity indexes (μ_2/Γ^2) of the SCL micelles and the non-cross-linked micelles were ~0.10 at pH 9.0. The almost constant $\langle R_h \rangle$ and polydispersity values of the PDEA-core micelles before and after cross-linking suggest that the cross-linking reaction takes place exclusively inside the PDMA inner layer and intermicellar cross-linking does not occur due to the steric repulsion imparted by the coronal PNIPAM chains.

Figure 5b illustrates the pH dependence of dynamic LLS results of the SCL micelles. In the pH range of 2−12, the scattered light intensity exhibits no appreciable changes. This further confirms that the shell cross-linking is successful.

Otherwise, the micelles will dissociate into unimers at acidic conditions, leading to a large decrease of scattered intensities. However, in the pH range of 6−8, $\langle R_h \rangle$ exhibits the most dramatic decrease. This is in agreement with the pK_a value of the PDEA homopolymers (~7.3). Further LLS studies revealed that the pH-dependent swelling/deswelling of the PDEA cores is fully reversible (Scheme 2). As most of the size changes take place around physiological pH's, this augurs well for the potential applications of such structurally stable SCL micelles in the field of nanosized drug delivery vehicles, which will exhibit the "triggered release" of the encapsulated hydrophobic drugs.

TEM images of the SCL micelles (Figure 6) revealed the presence of presumably spherical micelles of ~20−30 and ~25−40 nm in diameter at pH 9.0 and 5.0, respectively. The particle sizes estimated from TEM were systematically smaller than those obtained by dynamic LLS, which were ~48 and 76 nm in diameters for SCL micelles at pH 9.0 and 5.0, respectively. It is well-known that diameters measured by TEM are typically much smaller than those obtained by dynamic LLS because the former reflects conformations in the dry state, while the latter reflects the dimensions of both the PDEA core and the stretched PNIPAM coronas. The general agreement between sizes measured by dynamic LLS and TEM suggests that the spherical morphologies observed by TEM are present in solution. The presence of spherical morphologies for SCL micelles at pH 5.0 further confirms that the shell cross-linking has successfully fixed the micellar nanostructure.

It is well-known that the PNIPAM homopolymer undergoes a thermal phase transition in dilute aqueous solution above its LCST of ~32 °C.[67,68] At temperatures below the LCST, the PNIPAM chains adopt a randomly coiled structure due to the predominantly intermolecular hydrogen-bonding interactions between PNIPAM chains and water molecules. At temperatures above the LCST, intramolecular hydrogen-bonding interactions cause the chains to become compact and collapse, reducing their water solubility. As the obtained SCL micelles possess PNIPAM coronas, they should exhibit thermoresponsiveness.

Figure 7a shows the temperature dependence of average hydrodynamic radius, $\langle R_h \rangle$, of the SCL micelles in aqueous solution at an extremely low concentration (0.01 g/L, pH 9.0) during the heating process. Each data point was obtained after the measured values were stable. Upon heating, $\langle R_h \rangle$ decreases monotonically from 24 to 18 nm in the temperature range of 32−40 °C. The transition is relatively broad, spanning about 8 °C. For the PNIPAM homopolymers, individual PNIPAM chains free in solution usually exhibit an abrupt decrease of sizes in the narrow temperature range of 31−33 °C.[68] From Figure 7b, we can observe that scattered light intensity and polydispersity indexes (μ_2/Γ^2) of SCL micelles remain almost unchanged in the temperature range of 23−44 °C, indicating that the decrease of $\langle R_h \rangle$ above 32 °C should be ascribed to the intramicellar collapse of the PNIPAM corona.

Figure 8 shows the temperature dependence of transmittance at 500 nm for the SCL micelles prepared from the PDEA-*b*-PDMA-*b*-PNIPAM triblock copolymer at 5.0 g/L. The transmittance starts to decrease dramatically above 32 °C. This should be due to the aggregation of SCL micelles with collapsed PNIPAM coronas at relatively high concentrations. SCL micelles with collapsed PNIPAM coronas tend to collide with each other, which will surely contribute to the intermicellar aggregation because the PNIPAM corona becomes "sticky" above their LCST. The transmittance decreases from 80% at room temperature to ~20% at 40 °C (Figure 3). It should be noted that at a concentration of 5.0 g/L there is no apparent macroscopic phase
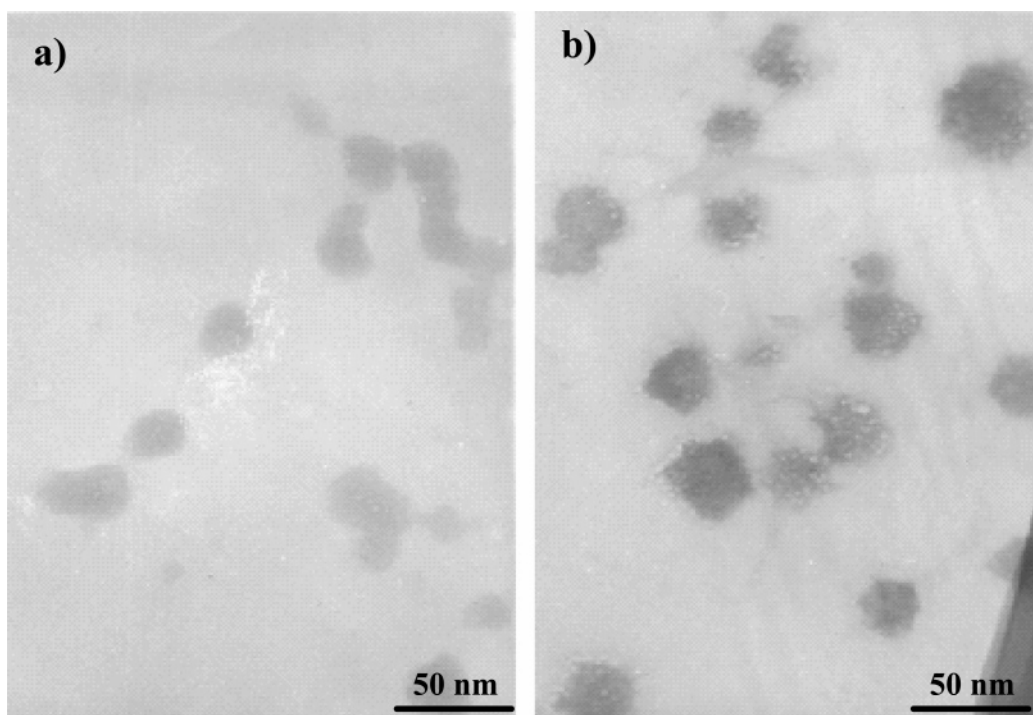
Figure 6. Typical TEM images obtained for SCL micelles of the PDEA-*b*-PDMA-*b*-PNIPAM triblock copolymer at (a) pH 9.0 and (b) pH 5.0. The target degree of shell cross-linking was 100%.
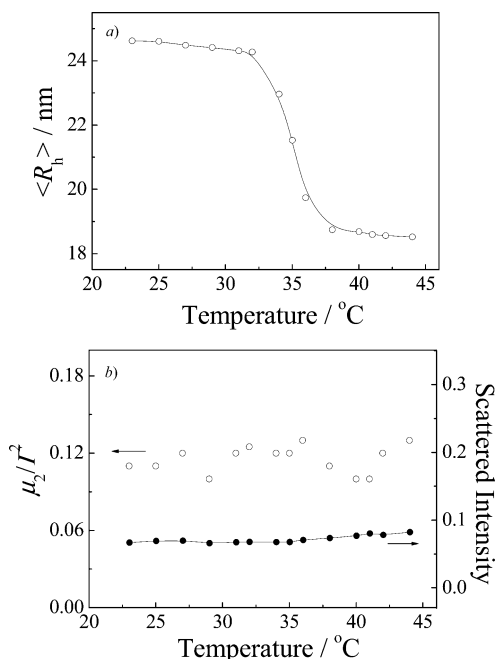

Figure 7. Variation of (a) intensity-average hydrodynamic radius, $\langle R_\mathrm{h} \rangle$, and (b) scattered light intensity and polydispersity index (μ_2/Γ^2) as a function of temperature at pH 9.0 obtained for a 0.01 g/L aqueous solution of SCL micelles of the PDEA-*b*-PDMA-*b*-PNIPAM triblock copolymer. The target degree of shell cross-linking was 100%.
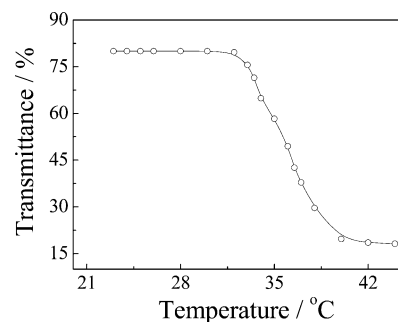

Figure 8. Temperature-dependent transmittance at pH 9.0 obtained for 5.0 g/L aqueous solutions of SCL micelles of the PDEA-*b*-PDMA-*b*-PNIPAM triblock copolymer. The target degree of shell cross-linking was 100%.

separation even after storage at 40 °C for 5 days. The different thermoresponsive collapse and aggregation behaviors at low and high concentrations (Figures 7 and 8) for SCL micelles prepared from PDEA-*b*-PDMA-*b*-PNIPAM might be further utilized to control the local concentrations and sizes of drug nanocarriers after being delivered to the target sites.

Theoretically, the thermal phase transition of the PNIPAM corona of SCL micelles at elevated temperatures will lead to changes of the permeability of the corona to guest molecules. Okano and co-workers[46,47] prepared polymeric micelles from diblock copolymers of PNIPAM and poly(butyl methacrylate) (PBMA) or polystyrene (PS). The hydrophobic drug, adriamycin (ADR), was loaded into the hydrophobic cores of micelles. As the micelle corona consists of thermoresponsive PNIPAM, they discovered that the releasing kinetics of ADR can be finely tuned by temperature, exhibiting a much enhanced release rate above the phase transition temperature of the PNIPAM corona. In their case, the micelles do not possess a stabilized structure; i.e., no cross-linking of the core or shell was performed. Moreover, a cosolvent approach is necessary to actuate the micelle formation, and the complete removal of organic solvent molecules through tedious and time-consuming dialysis is necessary. Finally, the micelle cores were essentially hydrophobic, and only water-insoluble drugs can be solubilized and delivered.

Drug Release from Shell Cross-Linked Micelles. Although various types of SCL micelles have been reported, very few studies concerning the drug release behavior have been reported.[69] It has been observed that the shell cross-linking can partially modify the release profile, but not that prominently, probably due to the fact that the guest molecules are typically much smaller than the pores of the cross-linked network within the shell. Thus, more controlling functions or components need
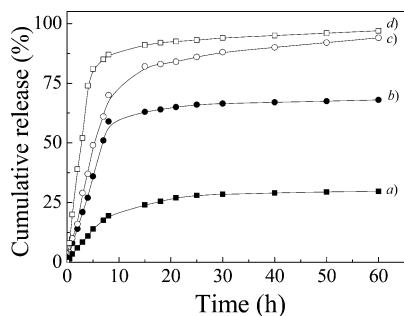
Figure 9. Cumulative DIP release from SCL micelles of PDEA-*b*-PDMA-*b*-PNIPAM solubilized with DIP within the PDEA cores (initially at pH 9.0) to buffer solutions: (a) at pH 8.0 and 25 °C; (b) at pH 8.0 and 37 °C; (c) at pH 5.0 and 25 °C; (d) at pH 5.0 and 37 °C.

to be introduced into SCL micelles to realize more sophisticated and smarter control over the release kinetics of encapsulated guest molecules.

We can expect that the SCL micelles fabricated from PDEA-*b*-PDMA-*b*-PNIPAM should prove to be excellent drug nanocarriers due to the following advantages. First, the structure of the nanocarrier is permanently stable, due to the introduction of shell cross-linking. Thus, the large dilution typically accompanying the administration process, the variations of pH, temperature, and ionic strengths, etc., will not disintegrate the micelle structure. Second, as the SCL micelles possess pH-responsive PDEA cores, the encapsulation and subsequent triggered release of drugs is possible.[45,70] Finally, the thermoresponsive PNIPAM corona of the obtained SCL micelles can be utilized to act as additional tuning parameters for the controlled and smart release of guest molecules, which is made possible by the smart changes of corona permeability upon thermal phase transitions.[46,47,71−74] We then tested the drug release profile at different pH's and temperatures after solubilizing a model hydrophobic drug, DIP, within the hydrophobic PDEA cores of SCL micelles fabricated from PDEA-*b*-PDMA-*b*-PNIPAM.

After mixing DIP with SCL micelles in aqueous solution at pH 4−5, DIP can be facilely loaded into the hydrophobic PDEA core of the SCL micelles upon adjusting the solution pH to 9.0 with NaOH. The drug release profiles at different pH's and temperatures were monitored using a conventional dialysis method. The amounts of released DIP in the external buffer solutions were determined based on a standard curve of DIP at a fixed pH of 3.0.

Figure 9 shows the time dependence of cumulative DIP release from drug-loaded SCL micelles into buffer solutions at different pH's and temperatures. When the drug-loaded SCL micelle solution was placed in a pH 8.0 buffer at 25 °C, only ∼25% of the loaded drug can be released even after 60 h. This is due to the fact that the PDEA core still remains hydrophobic, which can well solubilize the hydrophobic drug. This indicates that the PDEA core possesses a relatively high partition coefficient for DIP, as compared to that of the external buffer solution. Tang et al.[45] reported the release kinetics of DIP loaded within the PDEA core of the non-cross-linked micelles of PEG-*b*-PDMA-*b*-PDEA. In a buffer solution at pH 7.4, ∼45% of the loaded drug was released within 3 h. Two factors may contribute to the slow release observed in the current case. We used a buffer solution of 8.0, in which the PDEA core is becoming more hydrophobic. However, the shell cross-linking may also partially retard the drug release.

In a buffer solution at pH 8.0 and 37 °C, a much enhanced release rate of DIP can be observed compared to that at 25 °C.

Approximately 60% of loaded DIP was released within 8 h. Okano and co-workers[46] also observed that the release of ADR can be accelerated at elevated temperatures when the drug was loaded into the hydrophobic PBMA core covered with PNIPAM coronas. They ascribed this to the structural deformation of PBMA-core micelles. In the current case, dynamic LLS experiments of an extremely dilute aqueous solution (0.01 g/L) of the SCL micelles revealed that micelle radius decreases from 24 to 18 nm upon heating from 25 to 40 °C (Figure 7). The 6 nm size decrease should be due to the collapse of the thermoresponsive PNIPAM corona, leading to a much thinner micelle corona. Moreover, the collapse of the PNIPAM layer may also lead to the formation of pores or channels throughout the corona layer.[72] Both of these two factors will contribute to the enhanced permeability of the PNIPAM corona to guest molecules, leading to faster release of DIP.

When the buffer solution was at pH 5.0 (Figures 9c and 9d), even faster drug release can be typically observed. Depending on the solution temperature, ∼80−90% of the loaded drugs were released within the initial 10 h. At pH 5.0, the tertiary amine residues of the PDEA core were almost completely protonated, and the core is becoming hydrophilic, leading to its extensive swelling (Figure 5). Thus, the pH decrease of the buffer solution leads to the type of 'triggered' release of guest molecules.

A closer examination of Figures 9c and 9d tells us that at pH 5 the release rate at 37 °C is considerably faster than that at 25 °C, which could be due to the thermal phase transition of the PNIPAM corona, leading to enhanced permeability to drug molecules.

On the basis of the above discussion, we successfully established that the SCL micelles fabricated from PDEA-*b*-PDMA-*b*-PNIPAM can act as excellent drug nanocarriers, the structural integrity of which was endowed with the shell cross-linking. Moreover, as the SCL micelles possess pH-controllable core swellability and thermo-tunable corona permeability, the release profile of encapsulated guest molecules can be dually controlled by solution pH and temperature. In practice, most pathological processes exhibit either a slight increase in temperature or decrease in pH. For instance, contrary to the normal blood pH of 7.4, extracellular pH values in tumorous tissues are determined to be around 6.5−7.0. Moreover, drug nanocarriers can enter living cells via endocytosis, and the intracellular environment is typically acidic (pH 5−6). As the reported multiresponsive SCL micelles possess excellent structural stability and exhibit uniquely dual control (pH and temperature) of the drug release profile, they should act as suitable drug nanocarriers with more sophisticated and smarter controlled-release behavior in real-world clinical applications

Conclusion

The well-defined PDEA-*b*-PDMA-*b*-PNIPAM triblock copolymer was successfully synthesized via ATRP. The triblock copolymer can self-assemble into PNIPAM-core micelles at acidic pH's and elevated temperatures and PDEA-core micelles at alkaline pH's and room temperature. Dynamic LLS results indicated the presence of nearly monodisperse micelles in both cases, and the micellization was fully reversible. Novel SCL micelles with pH-responsive PDEA cores and thermosensitive PNIPAM coronas in aqueous solution were then fabricated by cross-linking the inner PDMA shells of the PDEA-core micelles. The reversible pH-dependent swelling/deswelling of PDEA cores and thermoresponsive collapse/aggregation of PNIPAM coronas of the resultant SCL micelles were investigated in some

detail. These SCL micelles can act as drug nanocarriers: loading the DEA cores with a hydrophobic drug, followed by change of solution pH and temperature, dually controlled rate of drug release of drug-loaded SCL micelles. This represents the first report of the preparation of multiresponsive SCL micelles, which could lead to more sophisticated, controllable, and smarter nanocarriers.

References and Notes

(1) Cölfen, H. *Macromol. Rapid Commun.* **2001**, *22*, 219−252.
(2) Rodríguez-Hernández, J.; Lecommandoux, S. *J. Am. Chem. Soc.* **2005**, *127*, 2026−2027.
(3) Arotçaréna, M.; Heise, B.; Ishaya, S.; Laschewsky, A. *J. Am. Chem. Soc.* **2002**, *124*, 3787−3793.
(4) Virtanen, J.; Arotçaréna, M.; Heise, B.; Ishaya, S.; Laschewsky, A.; Tenhu, H. *Langmuir* **2002**, *18*, 5360−5365.
(5) André, X.; Zhang, M. F.; Müller, A. H. E. *Macromol. Rapid Commun.* **2005**, *26*, 558−563.
(6) Alarcón, C. d. l. H.; Pennadam, S.; Alexander, C. *Chem. Soc. Rev.* **2005**, *34*, 276−285.
(7) Bütün, V.; Liu, S.; Weaver, J. V. M.; Bories-Azeau, X.; Cai, Y.; Armes, S. P. *React. Funct. Polym.* **2006**, *66*, 157−165.
(8) Liu, S. Y.; Armes, S. P. *Angew. Chem., Int. Ed.* **2002**, *41*, 1413−1416.
(9) Bo, Q.; Zhao, Y. *J. Polym. Sci., Part A: Polym. Chem.* **2006**, *44*, 1734−1744.
(10) Li, Y. T.; Armes, S. P.; Jin, X. P.; Zhu, S. P. *Macromolecules* **2003**, *36*, 8268−8275.
(11) Ma, Y. H.; Tang, Y. Q.; Billingham, N. C.; Armes, S. P.; Lewis, A. L.; Lloyd, A. W.; Salvage, J. P. *Macromolecules* **2003**, *36*, 3475−3484.
(12) Mountrichas, G.; Pispas, S. *Macromolecules* **2006**, *39*, 4767−4774.
(13) Pispas, S. *J. Polym. Sci., Part A: Polym. Chem.* **2006**, *44*, 606−613.
(14) Vamvakaki, M.; Palioura, D.; Spyros, A.; Armes, S. P.; Anastasiadis, S. H. *Macromolecules* **2006**, *39*, 5106−5112.
(15) Vandermeulen, G. W. M.; Tziatzios, C.; Duncan, R.; Klok, H. A. *Macromolecules* **2005**, *38*, 761−769.
(16) Zhang, W.; Shi, L.; Ma, R.; An, Y.; Xu, Y.; Wu, K. *Macromolecules* **2005**, *38*, 8850−8852.
(17) Schilli, C. M.; Zhang, M.; Rizzardo, E.; Thang, S. H.; Chong, Y. K.; Edwards, K.; Karlsson, G.; Müller, A. H. E. *Macromolecules* **2004**, *37*, 7861−7866.
(18) Liu, S. Y.; Billingham, N. C.; Armes, S. P. *Angew. Chem., Int. Ed.* **2001**, *40*, 2328−2331.
(19) Cai, Y. L.; Armes, S. P. *Macromolecules* **2004**, *37*, 7116−7122.
(20) Bütün, V.; Top, R. B.; Ufuklar, S. *Macromolecules* **2006**, *39*, 1216−1225.
(21) Saito, R.; Ishizu, K.; Fukutomi, T. *Polymer* **1990**, *31*, 679−683.
(22) Ishizu, K.; Onen, A. *J. Polym. Sci., Part A: Polym. Chem.* **1989**, *27*, 3721−3731.
(23) Wilson, D. J.; Riess, G. *Eur. Polym. J.* **1988**, *24*, 617−621.
(24) Guo, A.; Liu, G.; Tao, J. *Macromolecules* **1996**, *29*, 2487−2493.
(25) Ding, J. F.; Liu, G. *J. Phys. Chem. B* **1998**, *102*, 6107−6113.
(26) Stewart, S.; Liu, G. *Chem. Mater.* **1999**, *11*, 1048−1054.
(27) Thurmond Ii, K. B.; Huang, H.; Clark Jr, C. G.; Kowalewski, T.; Wooley, K. L. *Colloids Surf., B* **1999**, *16*, 45−54.
(28) Wooley, K. L. *J. Polym. Sci., Part A: Polym. Chem.* **2000**, *38*, 1397−1407.
(29) Liu, F.; Liu, G. *Macromolecules* **2001**, *34*, 1302−1307.
(30) Read, E. S.; Armes, S. P. *Chem. Commun.* **2007**, 3021−3035.
(31) Thurmond, K. B.; Kowalewski, T.; Wooley, K. L. *J. Am. Chem. Soc.* **1996**, *118*, 7239−7240.
(32) Thurmond, K. B.; Kowalewski, T.; Wooley, K. L. *J. Am. Chem. Soc.* **1997**, *119*, 6656−6665.
(33) Huang, H.; Kowalewski, T.; Remsen, E. E.; Gertzmann, R.; Wooley, K. L. *J. Am. Chem. Soc.* **1997**, *119*, 11653−11659.
(34) Bütün, V.; Billingham, N. C.; Armes, S. P. *J. Am. Chem. Soc.* **1998**, *120*, 12135−12136.

(35) Bütün, V.; Lowe, A. B.; Billingham, N. C.; Armes, S. P. *J. Am. Chem. Soc.* **1999**, *121*, 4288−4289.
(36) Bütün, V.; Wang, X. S.; de PazBanez, M. V.; Robinson, K. L.; Billingham, N. C.; Armes, S. P.; Tuzar, Z. *Macromolecules* **2000**, *33*, 1−3.
(37) Liu, S. Y.; Weaver, J. V. M.; Save, M.; Armes, S. P. *Langmuir* **2002**, *18*, 8350−8357.
(38) Liu, S. Y.; Weaver, J. V. M.; Tang, Y.; Billingham, N. C.; Armes, S. P.; Tribe, K. *Macromolecules* **2002**, *35*, 6121−6131.
(39) Li, Y.; Lokitz, B. S.; McCormick, C. L. *Macromolecules* **2006**, *39*, 81−89.
(40) Jiang, X. Z.; Luo, S. Z.; Armes, S. P.; Shi, W. F.; Liu, S. Y. *Macromolecules* **2006**, *39*, 5987−5994.
(41) Weaver, J. V. M.; Tang, Y. Q.; Liu, S. Y.; Iddon, P. D.; Grigg, R.; Billingham, N. C.; Armes, S. P.; Hunter, R.; Rannard, S. P. *Angew. Chem., Int. Ed.* **2004**, *43*, 1389−1392.
(42) Liu, S. Y.; Armes, S. P. *J. Am. Chem. Soc.* **2001**, *123*, 9910−9911.
(43) Lokitz, B. S.; Convertine, A. J.; Ezell, R. G.; Heidenreich, A.; Li, Y.; McCormick, C. L. *Macromolecules* **2006**, *39*, 8594−8602.
(44) Pilon, L. N.; Armes, S. P.; Findlay, P.; Rannard, S. P. *Langmuir* **2005**, *21*, 3808−3813.
(45) Tang, Y.; Liu, S. Y.; Armes, S. P.; Billingham, N. C. *Biomacromolecules* **2003**, *4*, 1636−1645.
(46) Chung, J. E.; Yokoyama, M.; Yamato, M.; Aoyagi, T.; Sakurai, Y.; Okano, T. *J. Controlled Release* **1999**, *62*, 115−127.
(47) Chung, J. E.; Yokoyama, M.; Okano, T. *J. Controlled Release* **2000**, *65*, 93−103.
(48) Ciampolini, M.; Nardi, N. *Inorg. Chem.* **1996**, *5*, 41−44.
(49) Muhlebach, A.; Gaynor, S. G.; Matyjaszewski, K. *Macromolecules* **1998**, *31*, 6046−6052.
(50) Davis, K. A.; Matyjaszewski, K. *Macromolecules* **2000**, *33*, 4039−4047.
(51) Lee, S. B.; Russell, A. J.; Matyjaszewski, K. *Biomacromolecules* **2003**, *4*, 1386−1393.
(52) Cai, Y. L.; Tang, Y. Q.; Armes, S. P. *Macromolecules* **2004**, *37*, 9728−9737.
(53) Karanikolopoulos, N.; Pitsikalis, M.; Hadjichristidis, N.; Georgikopoulou, K.; Calogeropoulou, T.; Dunlap, J. R. *Langmuir* **2007**, *23*, 4214−4224.
(54) Cai, Y. L.; Armes, S. P. *Macromolecules* **2005**, *38*, 271−279.
(55) Jin, X. P.; Shen, Y. Q.; Zhu, S. P. *Macromol. Mater. Eng.* **2003**, *288*, 925−935.
(56) Teodorescu, M.; Matyjaszewski, K. *Macromolecules* **1999**, *32*, 4826−4831.
(57) Xia, Y.; Yin, X.; Burke, N. A. D.; Stöver, H. D. H. *Macromolecules* **2005**, *38*, 5937−5943.
(58) Xia, Y.; Burke, N. A. D.; Stöver, H. D. H. *Macromolecules* **2006**, *39*, 2275−2283.
(59) Bütün, V.; Billingham, N. C.; Armes, S. P. *Chem. Commun.* **1997**, 671−672.
(60) Vamvakaki, M.; Billingham, N. C.; Armes, S. P. *Macromolecules* **1999**, *32*, 2088−2090.
(61) Lee, A. S.; Gast, A. P.; Butun, V.; Armes, S. P. *Macromolecules* **1999**, *32*, 4302−4310.
(62) Bütün, V.; Armes, S. P.; Billingham, N. C. *Polymer* **2001**, *42*, 5993−6008.
(63) Cau, F.; Lacelle, S. *Macromolecules* **1996**, *29*, 170−178.
(64) Nivaggioli, T.; Tsao, B.; Alexandridis, P.; Hatton, T. A. *Langmuir* **1995**, *11*, 119−126.
(65) Wanka, G.; Hoffmann, H.; Ulbricht, W. *Macromolecules* **1994**, *27*, 4145−4159.
(66) Hurter, P. N.; Scheutjens, J. M. H. M.; Hatton, T. A. *Macromolecules* **1993**, *26*, 5030−5040.
(67) Schild, H. G. *Prog. Polym. Sci.* **1992**, *17*, 163−249.
(68) Wang, X.; Wu, C. *Macromolecules* **1999**, *32*, 4299−4301.
(69) Li, Y.; Lokitz, B. S.; Armes, S. P.; McCormick, C. L. *Macromolecules* **2006**, *39*, 2726−2728.
(70) Licciardi, M.; Giammona, G.; Du, J.; Armes, S. P.; Tang, Y.; Lewis, A. L. *Polymer* **2006**, *47*, 2946−2955.
(71) Wei, H.; Zhang, X.-Z.; Zhou, Y.; Cheng, S.-X.; Zhuo, R.-X. *Biomaterials* **2006**, *27*, 2028−2034.
(72) Li, G. Y.; Shi, L. Q.; Ma, R. J.; An, Y. L.; Huang, N. *Angew. Chem.* **2006**, *118*, 5081−5084.
(73) Soppimath, K. S.; Tan, D. C.-W.; Yang, Y. Y. *Adv. Mater.* **2005**, *17*, 318−323.
(74) Gil, E. S.; Hudson, S. M. *Prog. Polym. Sci.* **2004**, *29*, 1173−1222.

BM700743H